ACS OMEGA

http://pubs.acs.org/journal/acsodf

Article

Fabrication of Sacha Inchi Oil-Loaded Microcapsules Employing Natural-Templated *Lycopodium clavatum* Spores and Their Pressure-Stimuli Release Behavior

Bunthoeurn Khann, Duangporn Polpanich,* Pakorn Opaprakasit, Yodsathorn Wongngam, Kamonchanok Thananukul, and Chariya Kaewsaneha*

Cite This: *ACS Omega* 2023, 8, 20937−20948

Read Online

ACCESS | Metrics & More | Article Recommendations | Supporting Information

ABSTRACT: Polymeric particles have attracted vast attention for use in various fields, especially as drug carriers and cosmetics, due to their excellent ability to protect active ingredients from the environment until reaching a target site. However, these materials are commonly produced from conventional synthetic polymers, which impose adverse effects on the environment due to their non-degradable nature, leading to waste accumulation and pollution in the ecosystem. This work aims to utilize naturally occurring *Lycopodium clavatum* spores to encapsulate sacha inchi oil (SIO), which contains active compounds with antioxidant activity, by applying a facile passive loading/solvent diffusion-assisted method. Sequential chemical treatments by acetone, potassium hydroxide, and phosphoric acid were employed to remove native biomolecules from the spores before encapsulation effectively. These are mild and facile processes compared to other synthetic polymeric materials. Scanning electron microscopy and Fourier-transform infrared spectroscopy revealed the clean, intact, and ready-to-use microcapsule spores. After the treatments, the structural morphology of the treated spores remained significantly unchanged compared to the untreated counterparts. With an oil/spore ratio of 0.75:1.00 (SIO@spore-0.75), high encapsulation efficiency and capacity loading values of 51.2 and 29.3%, respectively, were obtained. Using antioxidant assay (DPPH), the IC_{50} of SIO@spore-0.75 was 5.25 ± 3.04 mg/mL, similar to that of pure SIO (5.51 ± 0.31 mg/mL). Under pressure stimuli (1990 N/cm^3, equivalent to a gentle press), a high amount of SIO was released (82%) from the microcapsules within 3 min. At an incubation time of 24 h, cytotoxicity tests showed a high cell viability of 88% at the highest concentration of the microcapsules (10 mg/mL), reflecting biocompatibility. The prepared microcapsules have a high potential for cosmetic applications, especially as functional scrub beads in facial washing products.

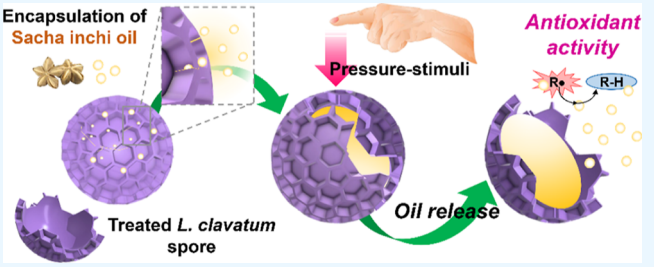

1. INTRODUCTION

Polymeric microcapsules have attracted vast attention for encapsulating active compounds in various applications, especially pharmaceutical products, drug delivery carriers, cosmetics, insecticides, paints, and textile products. These materials are mainly produced from conventional synthetic polymers, which impose adverse effects on the environment due to their non-degradable nature, leading to waste accumulation and contamination of the ecosystem. Developing "green" products with degradability from renewable raw materials instead of fossil-based resources has attracted vast attention in both research and commercial applications.[1−5]

Plant-based spores present one form of robust natural microcapsule templates for controlled-release systems. *Lycopodium (L.) clavatum* spores provide a readymade capsule scaffold with high structural uniformity, a large internal cavity, a porous shell, and a rigid outer shell structure that can stay intact in severe environments. They also highly resist strong acidic or basic environments and hardly dissolve in organic solvents. The spores comprise lipids, proteins, carbohydrates, and sporopollenin. Proteins are largely found in the spore's core, some known to cause allergy.[6] To prevent allergy problems, allergy-causing native biomolecules, i.e., proteins, are necessarily removed to create vacant space before encapsulating active ingredients in natural spores. Various chemical and enzymatic extractions can be used to extract these spores. Chemical extraction is an effective treatment method widely used to treat *L. clavatum*.[7,8] The process is based on sequential treatments with organic solvents, i.e., acetone, to remove lipids responsible for the hydrophobicity of the spores from the outer layer. An alkali solution is then used to remove proteins from the inner cavity, whereas aqueous acid treatment removes the

Received: March 14, 2023
Accepted: May 17, 2023
Published: May 31, 2023

polysaccharide intine, followed by a series of washing steps.[9−13] These are, however, mild processes (a temperature of <70 °C was applied in each step) compared to a one-pot method by using strong acids (i.e., hydrochloric acid and sulfuric acid) at a high treatment temperature of > 110 °C. The resulting clean microcapsule spores obtained using non-toxic mineral acids and alkalis are more suitable for cosmetic, pharmaceutical, and biomedical applications.

Various natural spores have been employed in encapsulating a wide range of active ingredients, e.g., drugs, vaccines, antibiotics, taste masking, oil, food supplement, and magnetic resonance imaging contrast agents, into the microcapsules.[7,14−18] Several encapsulation methods, e.g., vacuum, centrifugation, compression, and passive loading, have been developed to encapsulate various active ingredients into microcapsule spores.[3,19] Alpizar-Reyes et al. assessed the feasibility of using vacuum, passive, and centrifugated encapsulation techniques to load sunflower oil (rejuvenator) inside treated *L. clavatum* spores for asphalt self-healing.[19] The authors reported that a high encapsulation efficiency of 93.03% was obtained using vacuum encapsulation, followed by passive and centrifugal encapsulations (65.15 and 58.57%, respectively). The results are consistent with the fact that oil loading is influenced by the external energy supplied during the encapsulation process. In the case of passive loading, no external forces are involved, and loading is limited by oil passage into the internal cavity by nanoscale channels located on the spore wall.[4] Dyab et al. demonstrated an encapsulation of erythromycin and bacitracin antibiotics in natural spores using a passive diffusion followed by a vacuum loading technique.[18] These two antibiotics were successfully encapsulated with a loading capacity and entrapping efficiency of 16.2 and 32.4%, respectively.

Sacha inchi (*Plukenetia volubilis L.*), also known as Maní Inca, is a wild oleaginous plant of the *Euphorbiaceae* family, commonly grown in Central America. Sacha inchi oil (SIO) has aroused interest in the food and cosmetic industries because of an abundance of high-quality active ingredients in its seeds. Many studies have shown interest in this oil since its composition accounts for around 93% fatty acids, from which approximately 40−50% correspond to linolenic acid (omega-3), 30−40% to linoleic acid (omega-6), and ∼10% to oleic acid.[20,21] Natural antioxidants, including tocopherols isomers and polyphenolics, have also been found in the oil.[22] In vitro studies have shown that commercially available virgin SIO was not bactericides for *Staphylococcus (S.) aureus*. However, they were capable of preventing the attachment of *S. aureus* to keratinocytes and efficiently detaching *S. aureus* from human skin explants.[23] Recently, a clinical study to assess the moisturizing efficiency and skin irritation potential of SIO has been demonstrated. The results indicated that SIO is safe to use and provided evidence supporting the performance of the oil as an active moisturizing ingredient.[24−26] However, its use is constantly confronted by several factors, including its high volatility and high risk of deterioration upon direct exposure to heat, humidity, light, or oxygen. To overcome these limitations, polymeric nano/microparticles have been introduced to encapsulate oil, shielding them with good stability, controlled delivery, enhanced bioavailability, and improved efficacy. Recently, the encapsulation of SIO into various polymeric carriers has been developed by several research groups.[21,27−30] El Ghazzaqui Barbosa et al. fabricated SIO-encapsulated carboxymethylcellulose and lactoferrin by a complex coacervation.[30] This technique does not use harsh preparation conditions (such as high temperatures and organic solvents). However, this technique requires a special washing step by freezing in liquid nitrogen (−180 °C) and freeze-drying for 48 h to isolate the purified products from the reaction media. Silva et al. utilized a combination of encapsulation techniques (emulsification and ionic gelation) to produce SIO-encapsulated sodium alginate particles.[28] Not only was sodium alginate employed as an encapsulating/gelation agent but also nonionic surfactants (Tween 20 and 80) were used to obtain stable particles. The temperature of the emulsion process needed to be maintained at 3 °C. Moreover, uniform encapsulated polymer particles are difficult to produce with these techniques. A solvent diffusion method is an alternative method to produce the particles with high encapsulation efficiency and uniform particles. Based on this technique, hydrophobic molecules are dissolved in a proper solvent and then diffused into hydrophobic polymer particles with gentle stirring. After removing the solvent, monodisperse polymeric particles with high hydrophobic molecule loading are obtained.[31]

In this work, *L. clavatum* natural microcapsule spores are utilized to encapsulate SIO using a combination of the facile passive loading and solvent diffusion-assisted method. This method provides various benefits such as low operational cost, compatibility with labile materials, high stability and uniformity of the final products, and feasibility for continuous large-scale production. To produce intact, clean, and ready-to-use microcapsule spores, their native biomolecules, i.e., proteins, are removed before encapsulating active ingredients by sequential chemical treatments (organic solvent-base/acid treatments) using acetone, potassium hydroxide, and phosphoric acid followed by a series of washing steps. The chemical compositions and morphology of the treated spores are determined. An SIO solution (dissolved in ethanol) is quickly loaded into the treated spores, whose encapsulation efficiency and loading capacity are evaluated via a UV−vis spectrometer. The release behaviors of the oil from the microcapsules under pressure stimuli are investigated. Finally, the toxicity of the encapsulated spores to fibroblast cells is assessed and compared to the pristine spores.

2. EXPERIMENTAL SECTION

2.1. Materials. *Lycopodium clavatum* spores (average diameter of 25 μm) (Sigma-Aldrich, Analysis grade), ethanol (Carlo Erba Chemical, Analytical), acetone (Carlo Erba Chemical, Analytical), sodium hydroxide (Carlo Erba Chemical, Analytical), potassium hydroxide (Carlo Erba Chemical, Analytical), 85% *ortho*-phosphoric acid (H_3PO_4, Carlo Erba Chemical, Analytical), and 37% hydrochloric acid (Carlo Erba Chemical, Analytical) were used as received. Virgin SIO was purchased from Chanjao Longevity Company, Thailand. Deionized (DI) water was used throughout this work.

2.2. Chemical Treatment of Spores. Chemical treatments were applied to remove native compounds from the cavity and surfaces of the spores.[32,33] Briefly, *L. clavatum* spores (5.0 g) were first refluxed in acetone (250 mL) at 60 °C for 6 h. The dispersion was cooled down and filtered by using a vacuum filtration unit. After drying, the acetone-treated spores were refluxed in KOH (1 M, 250 mL) at 60 °C for 12 h. The dispersion of KOH-treated spores was kept warm, diluted with DI water, filtered, and substantially washed with hot water and ethanol. Finally, KOH-treated spores were refluxed with

https://doi.org/10.1021/acsomega.3c01698
ACS Omega 2023, 8, 20937−20948

H_3PO_4 (250 mL) at 60 °C for 30 h. After that, H_3PO_4-treated spore dispersion was sequentially washed with hot water, acetone, HCl (2 M), NaOH (2 M), water, acetone, and ethanol and dried at 60 °C in an oven for 24 h. The treated microcapsule spores were kept at room temperature for further characterization.

The chemical compositions of the native and treated spores in each step were analyzed by Fourier-transform infrared (FTIR) spectroscopy in an attenuated total reflection (ATR) mode (Thermo Scientific, Nicolet iS5). The measurements were conducted at a 2 cm^{-1} resolution with 32 scans. To verify the morphology and cavity of the spores, the samples were ground before examining by a field emission scanning electron microscope (FE-SEM; JEOL JSM7800F, JAPAN) with an acceleration voltage of 1 kV at different magnifications.

2.3. Encapsulation of SIO into Treated Microcapsule Spores. SIO was dissolved in ethanol (9 %v/v, 2 mL) and stirred for 5 min. The treated microcapsule spores (150 mg) were suspended in the SIO solution and vortexed for 5 min at 1000 rpm. The SIO:spore ratio was varied at 0.25:1.00, 0.50:1.00, 0.75:1.00, and 1.00:1.00 and coded as SIO@spore-0.25, SIO@spore-0.50, SIO@spore-0.75, and SIO@spore-1.00, respectively. The native spores were also used to encapsulate SIO using the same conditions. The mixture was then horizontally shaken (Heidolph model Rotamax 120) at 250 rpm at room temperature for 24 h. The SIO-encapsulated microcapsule spores (SIO@spore) were collected by filtering and washing with ethanol (9 %v/v) to remove free excess oils. Finally, the SIO-encapsulated microcapsule spores were dried using a freeze dryer at 0.75 mmHg for 24 h and stored at 4 °C before use.

The chemical compositions and morphology of the SIO@spore were determined by ATR-FTIR and FE-SEM, respectively. A confocal laser scanning microscope (CLSM; Olympus, Fluoview FV10i) was used to analyze the content and location of the oils loaded in the microcapsule spores by the dye tagging method. Fluorescein isothiocyanate (FITC) and Nile red (100 ppm, 200 μL) were employed by mixing with SIO and microcapsule spores and incubating for 24 h while shaking. After washing the excess dye, the sample was dropped onto a glass slide and covered with a cover slip. The morphology of the sample was examined under the following conditions: laser excitation line 405 nm (60%), 473 nm (50%), and 600 nm (50%) with a plan-Abochromat 63× 1/4 oil differential interference contrast (CID) M27 objective lens. The fluorescence signals from free and entrapped SIO in the microcapsule spores were collected by a photomultiplier tube equipped with the following emission filters: 416−477, 498−550, and 572−620 nm. All images were recorded by focusing on the inside section of the spores connecting thin glass slides and binding within the vent shield at 60×. The autofluorescence of the microcapsule spores might interfere with the signal of FITC-SIO and Nile red-SIO. Therefore, CLSM settings of the spores were fixed at the same condition as that of FITC-SIO-loaded spores and Nile red-SIO-loaded spores.

2.4. Encapsulation Efficiency and Loading Capacity. The encapsulation efficiency (% EE) and loading capacity (% LC) were determined by suspending SIO@spore (15.0 mg) in ethanol (98 %v/v, 50 mL), stirring for 60 min, and sonicating at 24% amplitude for 2 min with 3 cycles. The spores were then separated by filtration. The concentration of SIO remaining in the supernatant was measured by a UV−vis spectrometer at 290 nm. The % EE and % LC were calculated following eqs 1 and 2, respectively.[34]

$$\%\ \mathrm{EE} = \frac{W_f}{W_i} \times 100 \tag{1}$$

$$\%\ \mathrm{LC} = \frac{W_f}{W_{spore}} \times 100 \tag{2}$$

where W_i and W_f are the initial weight of SIO in the system and encapsulated SIO in microcapsules (mg), respectively. W_{spore} is the weight of the microcapsule spores (mg).

2.5. Stability of SIO-Encapsulated Microcapsule Spores in an Aqueous Medium. The dispersion of SIO@spore-0.75 (20.0 mg) in phosphate buffer solution (PBS, 20.0 mL) was poured into a dialysis bag (MW cutoff 5 kDa). Then, the dialysis bag was suspended in PBS (120 mL) under continuous stirring of 200 rpm at 32 °C. The aliquot (5 mL) was removed from PBS at specified intervals, e.g., 0.5, 1, 2, 3, 4, 24, 48, and 72 h. This was then analyzed with UV−vis spectroscopy, whose %SIO leakage was calculated by eq 3

$$\%\ \text{SIO leakage} = \frac{M_l}{M_t} \times 100 \tag{3}$$

where M_l and M_t are the mass of SIO leakage in the PBS medium and the mass of SIO encapsulated in microcapsule spores (obtained from % LC), respectively. After each withdrawal, an equivalent volume of fresh PBS media was filled into the PBS solution.

2.6. Control Release Behavior. The control release behavior of the resulting materials is examined. The SIO@spore-0.75 powder (300 mg) was placed on an elastomer film. The material was then gently pressed under an aluminum plate for various times, i.e., 1−11 min[35] A pressure of 1990 N/cm^3 was measured. After that, the film was dipped in ethanol (9 % v/v, 40 mL) and sonicated for 5 min. The mixture was then filtered by a nylon syringe filter (0.2 μm), and ethanol solution was added to the supernatant to maintain the sample volume. The concentration of the released SIO in the supernatant was measured by a UV−vis spectrometer at 290 nm, using eq 4.

$$\%\ \text{release of SIO} = \frac{M_2}{M_1} \times 100 \tag{4}$$

where M_1 and M_2 are the mass of SIO encapsulated in microcapsule spores (obtained from % LC) and released SIO in the supernatant, respectively.

2.7. Cytotoxicity Test. The cytotoxicity of the SIO-encapsulated microcapsule spores (SIO@spore-0.75), the treated microcapsule spores, and pure SIO were examined using an MTS cell proliferation assay. The fibroblast cell line (L929) (2×10^4 cells/100 μL/well) was seeded in a 96-well microplate (Corning, USA) with a complete (10% FBS-supplemented) high-glucose DMEM (Gibco, USA). After that, the microplate was incubated in a CO_2 incubator at 37 °C overnight to allow cell adhesion. The samples were dispersed in the complete DMEM at various concentrations, i.e., 0, 0.00001, 0.0001, 0.001, 0.01, 0.1, 1, and 10 mg/mL. Then, 100 μL of each sample, including control (complete DMEM), was added to the cells seeded in a 96-well plate. After incubation at each time point (24, 48, and 72 h), the cells were washed with plain DMEM 2 times. The complete DMEM (100 μL) was then added to each well. The MTS reagent (Promega, USA) (20 μL) was added to each well and incubated in a CO_2

https://doi.org/10.1021/acsomega.3c01698
ACS Omega 2023, 8, 20937−20948

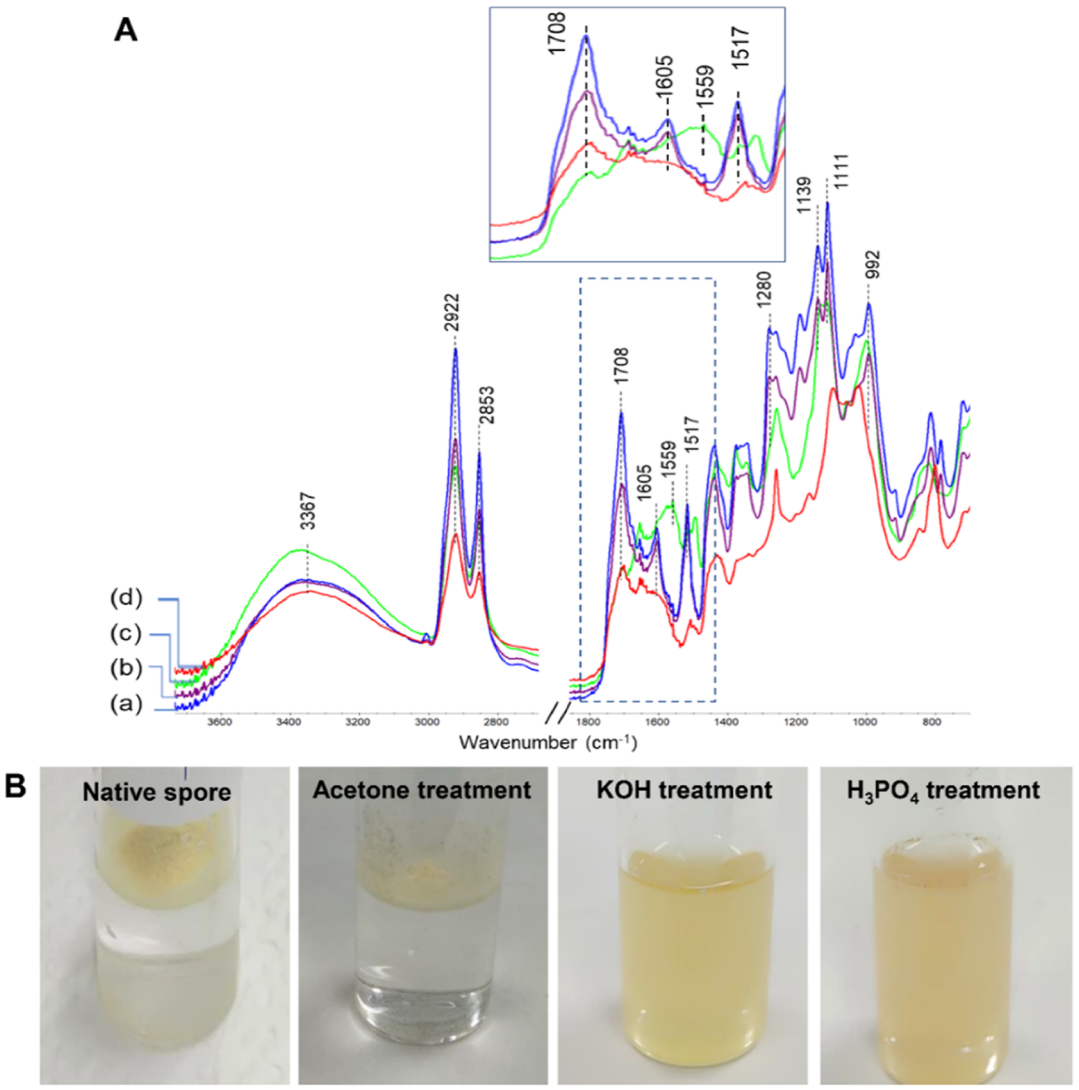

Figure 1. (A) ATR-FTIR spectra of (a) native spores and those after treatments by (b) acetone, (c) KOH, and (d) H_3PO_4. (B) Appearances of the spores subsequently treated with acetone, KOH, and H_3PO_4 dispersed in an aqueous phase compared to the native spores.

incubator at 37 °C for 2 h in the dark. All reactions for control and experiment samples were performed in triplicate. The absorbance at 490 nm was measured to quantify formazan products and at 630 nm was measured to subtract interferences using a multi-mode microplate reader (BioTek, USA). In addition, the morphological change of L929 cells was monitored using an optical microscope (OM) (Olympus, Japan) after incubating the cells with a given concentration of SIO@spore-0.75, the treated spores, and pure SIO.

3. RESULTS AND DISCUSSION

3.1. Characterization of Treated *L. clavatum* Spores.

As native *L. clavatum* spores are plant-based materials consisting of sporopollenin, lipids, proteins, and carbohydrates, chemical treatments are employed to remove small extractable molecules. ATR-FTIR analysis was used to determine chemical changes of the treated spores at a specific step. The results are shown in Figure 1A.

The native spores [spectrum (a)] show a broad band at 3367 cm^{-1}, corresponding to the O−H stretching modes of carboxylic acids, alcohol, and phenol. The two sharp bands at 2922 and 2853 cm^{-1} correspond to the asymmetric and symmetric C−H and CH_2 stretching modes of $-CH_2-$ groups, respectively. The band at 1708 cm^{-1} is assigned to the C═O stretching vibration of carboxyl groups, while that at 1517 cm^{-1} is due to the C═C mode of phenolic components. The 1437 cm^{-1} band is attributed to the C−H bending vibration of the $-CH_3$ group in carbohydrate structures. The C−O stretching mode of the carbohydrates appears at 1280 cm^{-1}. The bands at 1139 and 1111 cm^{-1} are C−H vibrations of aromatic rings in the sporopollenin. The characteristic modes of proteins (amide I at 1605 cm^{-1} and amide II at 1517 cm^{-1}) can be detected by ATR-FTIR spectroscopy.[36] According to previous work, acetone was used to solubilize unsaturated phospholipids from the spores. Slight changes in the spectra of acetone-treated spores [spectrum (b)] and native spores [spectrum (a)] were observed. The KOH treatment [spectrum (c)] could remove some proteins and hydrolyze esters to carboxylic acid salts. This leads to a disappearance of the characteristic bands of proteins at 1605 and 1517 cm^{-1} (C−N and C−N−C═O, respectively) and an appearance of the COO^- band at 1559 cm^{-1}. After H_3PO_4 treatment [spectrum (d)], the residual proteins were entirely removed, and protonation of nucleophilic groups may occur. The bands at

https://doi.org/10.1021/acsomega.3c01698
ACS Omega 2023, 8, 20937−20948

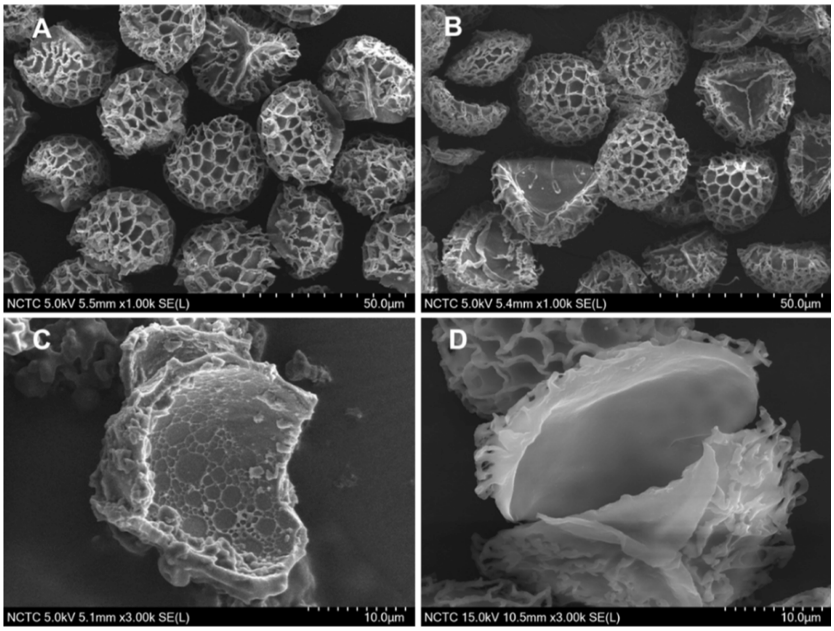

Figure 2. SEM images of external and inside cavities of native *L. clavatum* spores (A,C) and the treated *L. clavatum* spores (B,D).

1280 cm^{-1} corresponding to the C−O stretching of carbohydrates and 1517 cm^{-1} originating from phenolic components could not be detected after 30 h.[37]

The dispersibility in an aqueous medium of the spores from each treatment step is evaluated, as shown in Figure 1B. Acetone treatment was applied to solubilize unsaturated phospholipids from the spores. After the treatment, the treated spores still showed water-repellent (hydrophobicity) properties, similar to native spores, as this does not significantly alter the surface functionality. The KOH treatment removed proteins and hydrolyzed esters to carboxylic acid salts. This led to a significant improvement in the dispersibility of the treated spores in an aqueous phase. In the further treatment steps using an acid solution, the residual proteins were removed, and protonation of nucleophilic functional groups resulted in homogeneous dispersion of the spores.

The structure and morphology of the treated spores are determined by SEM, compared to the native spores, as shown in Figure 2. The native spores (Figure 2A) possess a spherical shape, with an average diameter of 28.90 ± 1.45 μm. A rough surface pattern and uniform ridges distributed on their surface were observed. After the chemical treatments (Figure 2B), no apparent changes in the external structure of *L. clavatum* spores were observed. This confirms that their cellulose shell structures are highly stable and can resist intense chemical and high-temperature environments.[32]

To determine the inside structure of the spores, the samples were broken by mechanical grinding before morphological investigation. The inside structure of the native spores is highly porous, with some small particles (Figure 2C). These agreed well with a previous study that the core of natural spores contains various materials, such as cytoplasm, lipids, and proteins.[35] In contrast, the treated spores reveal a clean cavity without other small particles (Figure 2D). This confirms that the treatments effectively removed unwanted molecules from the spores, generating microcapsule spores suitable for encapsulating active compounds.[3,4,9,37,38]

3.2. Encapsulation of SIO into the Treated Microcapsule Spores. SIO is encapsulated into the treated microcapsule spores using facile passive encapsulation and solvent diffusion-assisted methods to protect the oil from external environments. The treated spore and the active compound are mixed, and SIO is absorbed through the porous walls into the inner cavity of the treated spores by capillary action.[7,14] Barrier et al. reported that *L. clavatum* spores could encapsulate lipophilic liquids with low viscosity, e.g., cod liver oil and molten cocoa butter, and also small molecules with differing polarities without a significant harmful effect to them. It was observed that the chemical and physical features of the nano-sized channels present in *L. clavatum* could permit passage of a variety of polar and non-polar materials with sizes (Stokes' radius) up to 30 nm.[14] Mixtures of the microcapsule spores and SIO at desired ratios were prepared by a vortex mixer, followed by horizontal shaking for 24 h, to allow the loading saturation. The properties of the SIO-encapsulated microcapsule spores (SIO@spore), i.e., encapsulation efficiency (% EE), loading capacity (% LC), and morphology, were examined. The % EE and % LC values were measured using UV−vis spectroscopy, as shown in Figure 3.

To confirm the importance of the chemical treatments in removing native compounds and creating clean cavity microcapsules, the native spores were also used to encapsulate SIO, compared with the treated spores. At the same SIO/spore ratios of 0.25:1.00, 0.50:1.00, and 0.75:1.00 (Figure S1), the encapsulated microcapsules using a native spore as a template showed lower % EE and % LC values than those of the treated spores. When the SIO/native spore ratio was increased, no significant changes in the % EE and % LC values were observed. This confirms the hypothesis that the extraction treatment plays a key role in enhancing the loading efficiency of the active ingredients. In the case of using the treated spore as a template, with increasing SIO/spore ratio, the % EE and % LC values of the SIO@spore linearly increased, with the highest values of 51.2 ± 5% and 29.3 ± 2%, at a ratio of 0.75:1.00. A further increase in the ratio to 1.00:1.00, however, did not significantly improve the % EE and % LC values (52.2 ± 4% and 28.1 ± 3%, respectively). The encapsulation of SIO into the treated microcapsule spores is controlled by its

https://doi.org/10.1021/acsomega.3c01698
ACS Omega 2023, 8, 20937−20948

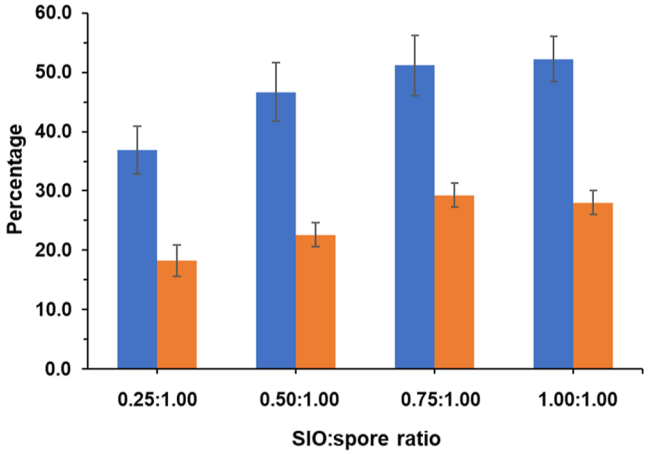

Figure 3. % EE and % LC values of the prepared SIO@spore with different SIO/spore ratios, i.e., 0.25:1.00, 0.50:1.00, 0.75:1.00, and 1.00:1.00.

diffusion through the nanochannel of the wall surface of the microcapsule spores. The major components of SIO are small-sized fatty acids, such as hexadecanoic acid (palmitic acid), 9,12-octadecadienoic acid (linoleic acid), 9-octadecenoic acid (oleic acid), and γ- and α-tocopherol, as summarized in Table S1 (see the Supporting Information). These small molecules can easily penetrate the nanosized pores of the microcapsule spores (<20 nm).[35] From passive loading mechanisms, no external force is involved. Loading is limited by the molecule passage into the internal cavity through nanochannels located on the spore's wall and the cavity's capacity.[4] Moreover, the high solubility of these small molecules in ethanol, with low viscosity, also contributes to the effectiveness of the encapsulation process. Likewise, the encapsulation of hydrophobic molecules into a hydrophobic polymer matrix occurs via the solvent diffusion method. The solvent plays many roles, e.g., in the swelling of polymer particles, diffusion of hydrophobic molecules from the solution into particles, and entrapment of molecules after solvent removal.[31]

It is known that unsaturated fatty acids such as linoleic and oleic acids possess antioxidant activity.[39] Moreover, tocopherol molecules in the SIO could play a major role in radical scavenging capacity. The results showed that % DPPH antioxidant activity (% inhibition) of the SIO@spores at a ratio of 0.75:1.00 (SIO@spore-0.75) increased with its concentration, as summarized in Figure S2. The IC_{50}, a concentration of a substance required to scavenge 50% of the initial DPPH radicals, of SIO@spore-0.75 was 5.25 ± 3.04 mg/mL, similar to that of pure oil (IC_{50} 5.51 ± 0.31 mg/mL). The tocopherol molecules comprise a chromane ring with hydroxyl groups that can donate hydrogen radicals to other free radicals in the system. This may minimize lipid peroxidation and harmful reactive oxygen species (ROS) in human cells. Furthermore, a hydrophobic side chain of tocopherols can be incorporated into cell membranes to protect them from oxidative damage.[40] Apart from the intrinsic properties of SIO, the outer protective layer of the treated *L. clavatum* spores is composed of sporopollenin, which is a biopolymer conjugated with phenolic compounds. This may partly play some role in the antioxidant activity of SIO@spore-0.75.[41]

The prepared SIO@spore prepared at a ratio of 0.75:1.00, coded as SIO@spore-0.75, was selected for further examination due to its highest % LC value. The morphology of the prepared SIO@spore-0.75 before and after tracking with FITC and Nile red was examined by SEM and CLSM, as shown in Figure 4. SIO@spore-0.75 maintained its structure and morphology without breaking (Figure 4A). No residues were observed on the particle's surface. The presence of bioactive SIO molecules inside the cavity of microcapsule spores was confirmed by CLSM. The images were recorded by focusing on the middle hole of the spores fixed between thin glass slides and inserted within the VECTASHIELD at 60×. Native *L. clavatum* spores (Figure 4B) showed autofluorescence with green color due to the cytoplasm inside the spores.[42−44] After the chemical treatments of the spores to remove these molecules, a hollow structure was generated (Figure 4C). Upon loading SIO into the treated spores (Figure 4D), encapsulated microcapsule spores with obscure green color inside the particle were observed, which likely originated from

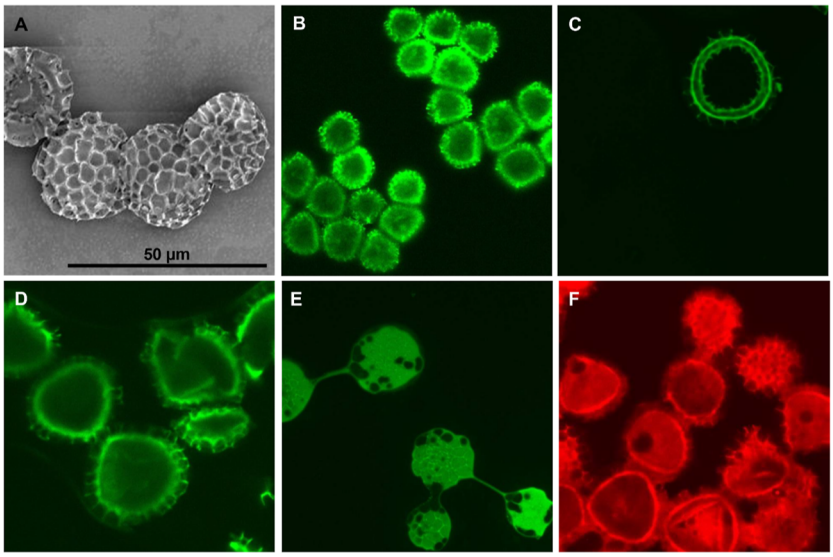

Figure 4. SEM images of the prepared SIO@spore-0.75 (A) and CLSM images of natural *L. clavatum* spores (B), treated spores (C), SIO@spore-0.75 (D), FITC-SIO@spore (E), and Nile red-SIO@spore (F).

https://doi.org/10.1021/acsomega.3c01698
ACS Omega 2023, 8, 20937−20948

the autofluorescence of pure SIO, as presented in Figure S3. Moreover, the particles were stained with FITC (Figure 4E). The bright green color was seen throughout the particles. In the case of the particles stained with Nile red (Figure 4F), the bright red color in the spores' cavity was displayed. Interestingly, the red color of each capsule spore illustrates different degrees of brightness. This likely reflects the different concentrations of Nile red dye and SIO located in the microcapsules. These imply that SIO active ingredients were successfully encapsulated into the treated microcapsule spores via a combination of simple passive encapsulation and solvent diffusion-assisted mechanisms.

FTIR spectroscopy was also applied to confirm the presence of SIO in the microcapsule spores. The spore samples were broken by mechanical gridding to reveal their inside structure, whose FTIR spectra were then recorded, as shown in Figure 5.

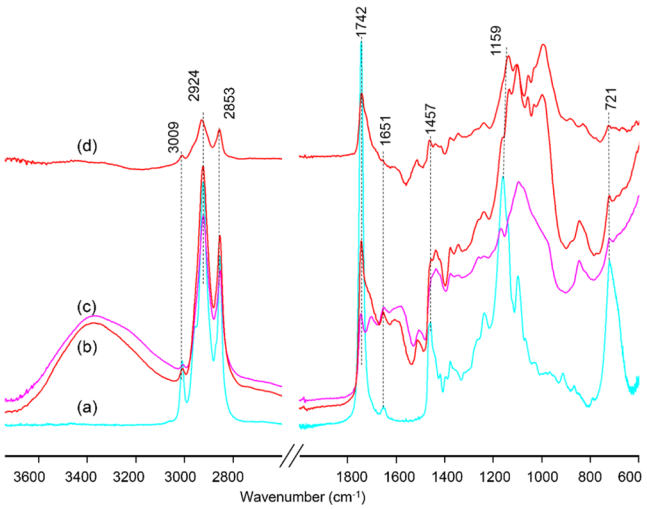

Figure 5. ATR-FTIR spectra of SIO@spore-0.75 (b) compared with its pure SIO (a) and starting treated spore (c) counterparts, and its corresponding difference spectrum (d) after subtraction by the starting treated spore.

SIO (spectrum a) shows a band at 3009 cm^{-1}, corresponding to the stretching mode of *cis* olefinic C−H. The bands at 2924 and 2853 cm^{-1} correspond to the methylene asymmetric and symmetric vibration, respectively. An intense band at 1742 cm^{-1} is assigned to the C═O stretching mode of ester groups, the characteristic of triacylglyceride oils. A weak band at 1651 cm^{-1} corresponds to the di-substituted *cis* C═C of the unsaturated acyl groups, whereas the band at 1457 cm^{-1} is assigned to the bending vibrations of CH_2 and CH_3 aliphatic groups. The results correlate well with those previously reported in the literature.[45] A band at 1159 cm^{-1} is attributed to the stretching vibrations of the C−O in the ester groups and to the bending vibration of the CH_2 group. The 721 cm^{-1} band is associated with an isolated *trans* alkene group (−HC═CH−). To examine in more detail, a difference spectrum was generated by subtracting the spectrum of the starting treated spore from SIO@spore-0.75, as shown in the spectrum (d). Positive difference bands were observed at the frequencies similar to the characteristic mode of SIO at 3009, 2924, and 2853 cm^{-1} (C−H stretching of the *cis* alkene group), at 1742 cm^{-1} (a strong band of the stretching vibration of C═O), and a band at 1159 cm^{-1} of C−O groups. The results confirm that SIO was successfully encapsulated into the microcapsule spores by this facile passive encapsulation.

3.2.1. Stability of the SIO-Encapsulated Microcapsule Spores. As the microcapsule spores are intended for use as a protective shell for SIO from environmental factors, especially UV light in cosmetic products, the SIO-encapsulated spores (SIO@spore-0.75) were directly exposed to UV light. The sample was placed under a UV lamp (UVA and UVB) at a distance of 20 cm under accelerated conditions (UV intensity of 0.6 mW/cm^2).[46,47] The stability of the encapsulated microcapsule spores in avoiding possible breakage, which may affect the material's practical use, was assessed. The shape and morphology of SIO@spore-0.75 were examined after UV treatment by SEM, as shown in Figure 6A. The encapsulated microcapsule spores retained their original morphology after UV exposure for 336 h, without damage or distortion, reflecting that the UV radiation has negligible effects on their shell structures.

The UV resistance performance of SIO@spore-0.75 was investigated using ATR-FTIR spectra as a function of the exposure time to intense UV radiation, as shown in Figure S4. At an interval time, the SIO@spore-0.75 was crushed, and their spectra were recorded. All spectra show slight changes in their characteristic bands, reflecting subtle changes in the chemical structures of the spore's shell and/or the loaded SIO. The corresponding spectra of pure SIO as a function of the UV exposure time were also examined, as shown in Figure S4. To precisely examine the changes in their chemical structures, difference spectra were generated by subtracting the starting materials (SIO@spore-0.75 or pure SIO) from their corresponding samples after UV exposure for 336 h. The difference spectra are compared in Figure 6B. For SIO, weak positive difference bands were observed at 3435 (O−H stretching of acids), 1725 (C═O stretching of carboxylic acid), and 985 and 950 cm^{-1} (asymmetric ring deformation of epoxides). Negative difference bands were observed at 3024 (═C−H stretching) and 1745 cm^{-1} (C═O stretching of ester groups). The results indicate the breaking of ester bonds of triglycerides, leading to the formation of free fatty acids and the conversion of unsaturated C═C bonds to epoxides due to oxidation reactions. The corresponding difference spectrum of SIO@spore-0.75, however, differs from that of pure SIO, with weak negative bands at 2925 and 2855 (C−H stretching), 1740 (aromatic esters), 1164 (C−O−C stretching), and 974 cm^{-1} (C−H bending in aromatic rings). This implies the conversion of aromatic or conjugated structures in the spore's shell, leading to the formation of aromatic acids, reflected by a positive difference band at 1704 cm^{-1}. The absence of changes in the SIO characteristic bands firmly indicates that SIO is effectively protected during this intense UV exposure.

To assess the stability of the SIO@spore-0.75 products in practical use, the leakage of SIO from the microcapsule spore in an aqueous medium (PBS solution) was examined by UV−vis spectroscopy, as summarized in Figure 6C. After 72 h of immersion in PBS at room temperature, a small amount of SIO (~0.4% wt) was detected. As previously mentioned, the SIO solution diffused into the treated spores through the nanochannel of the wall surface until it reached equilibrium. Although the surface of the microcapsule spores is not covered after loading, the hydrophobic SIO molecules may bind strongly with the inner wall of the treated spores, preventing their leakage from the microcapsules.[48] It was also reported that during the loading of many common compounds, a

https://doi.org/10.1021/acsomega.3c01698
ACS Omega 2023, 8, 20937−20948

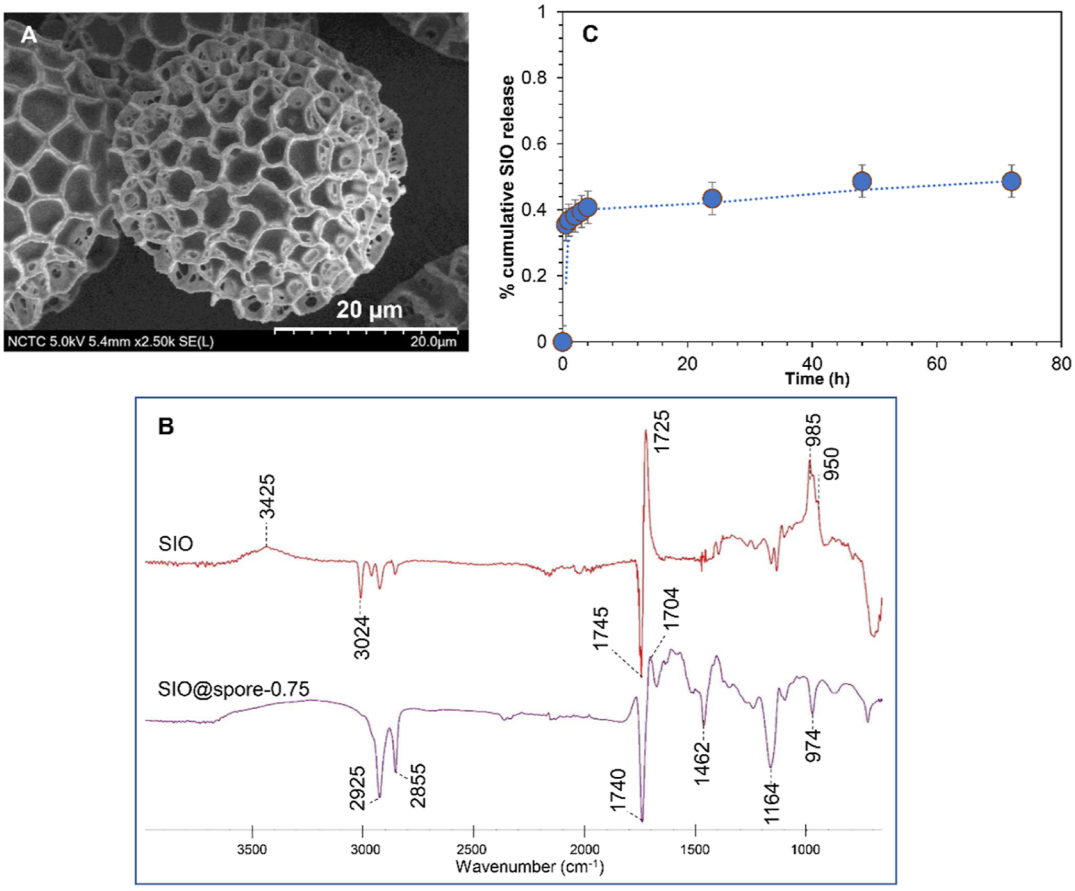

Figure 6. SEM image of SIO@spore-0.75 after UV exposure for 336 h (A) and ATR-FTIR difference spectra of SIO@spore-0.75 and pure SIO after subtraction of their corresponding starting sample from that after 336 h of UV exposure time (B). The % cumulative release of SIO from the SIO@spore-0.75 in PBS (C).

portion of the loaded compounds might bind to the encapsulant and cover its external surfaces.[11] Alpizar-Reyes et al. demonstrated that the presence of free oils on the surface of microcapsule spores could prevent the loaded oils from being lost through leaching.[19,49]

3.2.2. Release Behavior. The release behavior of SIO@spore-0.75 due to pressure stimuli (friction) was examined to assess its potential use in personal care (active scrub microbead) applications. The pressing time was varied from 1 to 11 min under a fixed pressure of 1990 N/cm^3. The release profiles of SIO from the SIO@spore-0.75 is shown in Figure 7. A burst release with a high amount of oil (81.62 ± 8.83%) was observed after applying the pressure for 3 min. The release of SIO might be mainly due to spores breaking under the applied pressure, as illustrated in Figure 8. This is consistent with the SEM results, in which the breaking of the microcapsule spore structure was observed by applying pressure (3 min). After that, a sustained release was observed. A complete release was detected after 7 min of pressure. The release behavior of SIO@spore under pressure stimuli is suitable for practical use in personal care (active scrub microbead) applications.

3.2.3. Cytotoxicity Property. The cytotoxicity of the encapsulated spores (SIO@spore-0.75), compared with the treated spores and pure SIO, was examined using an MTS assay, as summarized in Figure 9. After incubation with pure SIO for 24, 48, and 72 h (see Supporting Information, Figure S5), the viability of L929 cells was significantly decreased compared to the control (0 mg/mL oil in the complete

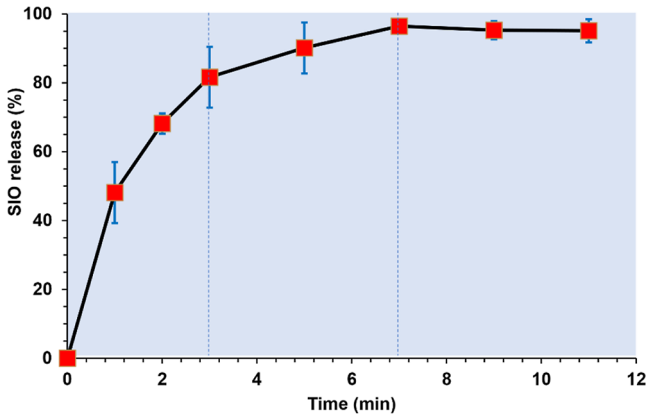

Figure 7. Release profile of SIO from SIO@spore-0.75 as a function of pressing times at a constant pressure of 1990 N/cm^3.

medium). The results demonstrate that a higher concentration of SIO significantly decreased cell viability, indicating that pure SIO is quite toxic to the cells. However, after encapsulating SIO into the treated spores at various loading times (Figure 9), the viability of L929 cells decreased slightly compared to the control. The results demonstrate that including SIO at a high concentration in the form of SIOs@spore only slightly decreased cell viability. The value was still higher than 70% at a concentration as high as 1 mg/mL, when incubated for 72 h. The results agree with that of the treated spores (see

https://doi.org/10.1021/acsomega.3c01698
ACS Omega 2023, 8, 20937−20948

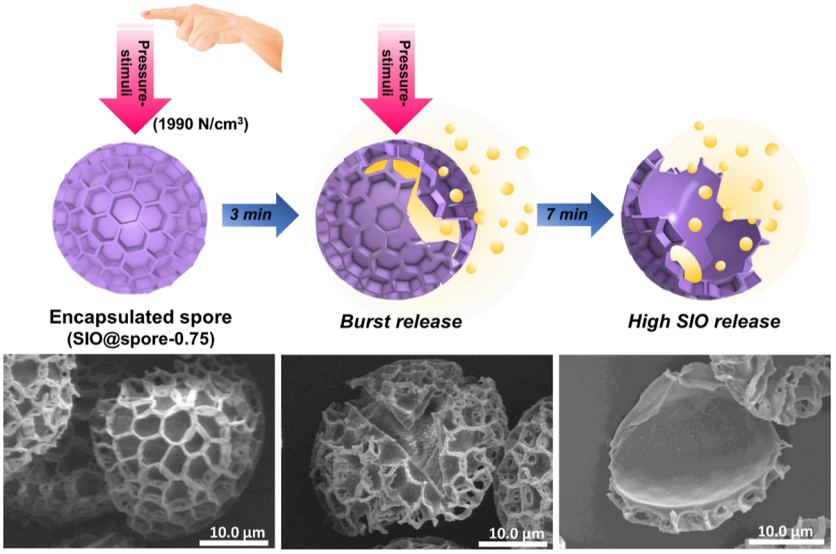

Figure 8. Proposed release mechanism of SIO from the encapsulated spores under pressure stimuli (after applying the pressure for 3 and 7 min) and SEM images of the spore's structure at each step.

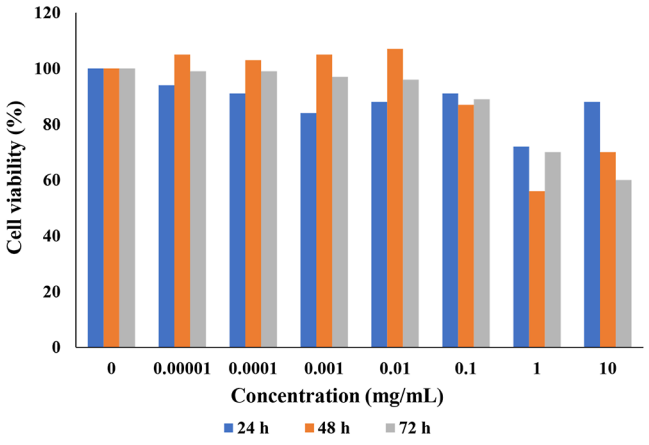

Figure 9. Viability of L929 cells after incubation with SIO@spore-0.75 with various concentrations (0−10 mg/mL) for 24, 48, and 72 h.

Supporting Information, Figure S6), whose viability of L929 cells slightly decreased. Also, a high cell viability of >70% was observed when incubated for 72 h. Moreover, it was found that the viability of L929 cells was higher than 100% at low concentrations when incubated with SIO@spore-0.75 for a long time (48 and 72 h). By considering the growth of L929, the doubling period of the cells reported by several authors is approximately 14 and 24 h.[50,51] It is possible that, at a long incubation time (48 and 72 h), the healthy living cells can proliferate, resulting in an increasing number of cells and % cell viability. These results can help support the compatibility of SIO@spore-0.75 at a certain concentration to the fibroblast cells after a long exposure time. This was higher than that of cells incubated with SIO for a short time (24 h).

Moreover, to confirm the biocompatibility of SIO@spore-0.75, the cell growth morphology was examined using OM at 10× magnification. The images were captured from each sample 48 h after incubating L929 cells with SIO@spore-0.75 at different concentrations. At low concentrations of SIO@spore-0.75 (0.00001−0.1 mg/mL, Figure 10B−F), no significant differences in cell confluency and morphology were observed compared to the control (Figure 10A). At 1 mg/mL SIO@spore-0.75 (Figure 10G), although the number of cells decreased, the well-morphology of the cells was still observed. At the highest concentration of 10 mg/mL (Figure 10H), the morphology of cells was not clearly detected due to the high amount of particles. The results are consistent with the cell incubated with the treated spores (see Supporting Information, Figure S7). In contrast, the morphology of cells incubated with pure SIO (see Supporting Information, Figure S8) showed significant differences in cell confluency and morphology in each dilution titer compared to the control. The number of cells was decreased when incubated with a low dilution titer. At the lowest dilution titer of 1:20 and 1:40 of the oil, the cells died due to the toxicity of the oil at high concentrations. The results of cell morphology are correlated well with the cell viability from MTS. The IC_{50} values (concentrations of the substances that exhibited 50% cell viability) of SIO@spore-0.75 and the treated spores were higher than 10 mg/mL, reflecting the high compatibility of these two materials with the cells. In contrast, the IC_{50} of pure SIO was 1:1280 of dilution titer, indicating potential cytotoxicity.

4. CONCLUSIONS

L. clavatum microcapsule spores were successfully used as a microcarrier template to encapsulate SIO using a combination of facile passive loading and solvent diffusion-assisted methods. Before encapsulation, sequential chemical treatments by acetone, potassium hydroxide, and phosphoric acid effectively removed protein molecules from the spores. These also led to the hydrolysis of esters and protonation of nucleophilic functional groups, generating surface charges which improve the dispersibility of the spores in the aqueous phase. Even after using sequential chemical treatments, the structural morphology of the treated spores remained significantly unchanged compared to that of the untreated counterparts. By varying SIO/spore ratios, the ratio of 0.75:1.00 (SIO@spore-0.75) provided the highest encapsulation efficiency values of 51%. The CLSM results confirmed that SIO is successfully encapsulated in the treated spores. The SIO passage into the internal cavity by nanochannels located on the spore wall,

https://doi.org/10.1021/acsomega.3c01698
ACS Omega 2023, 8, 20937−20948

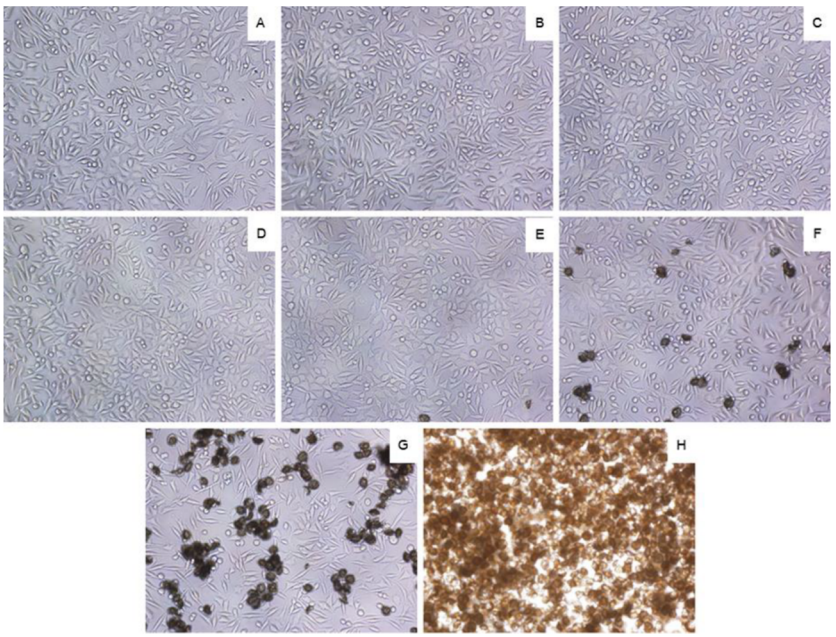

Figure 10. Microscopic examination of L929 cells at 48 h after incubation with SIO@spore-0.75 at 0, 0.00001, 0.0001, 0.001, 0.01, 0.1, 1.0, and 10 mg/mL, refer to (A−H), respectively.

combined with the diffusion of ethanol, contributes to the effectiveness of the encapsulation process. The *L. clavatum* spores act as a protective shell to prevent SIO degradation under UV light. Under applied pressure, SIO was burst released (82%) from the spores within 3 min, and approximately 96% of the oils were released within 7 min. The presence of tocopherol molecules in the SIO contributes to its DPPH antioxidant activity. In terms of toxicity, the results from MTS and morphological observations of SIO@spore-0.75 incubating with L929 cells showed that the particles were not toxic to the cells and presented IC_{50} of >10 mg/mL. The synthesized SIO@spore is highly promising for personal care products.

■ ASSOCIATED CONTENT

Supporting Information

The Supporting Information is available free of charge at https://pubs.acs.org/doi/10.1021/acsomega.3c01698.

% EE and % LC values of the prepared SIO@native spore with different SIO: native spore ratios, i.e., 0.25:1.00, 0.50:1.00, and 0.75:1.00, chemical compositions of commercial SIO determined by GC−MS analysis, DPPH antioxidant activity of pure SIO and SIO@spore-0.75, fluorescence intensity of SIO at a wavelength of 200−800 nm measured using fluorescence spectroscopy (PerkinElmer, LS55), ATR-FTIR spectra of SIO@spore-0.75 and SIO as a function of UV exposure time at accelerated conditions, viability of L929 cells after incubation with pure SIO at various concentrations (0−10 mg/mL) for 24, 48, and 72 h, viability of L929 cells after incubation with the treated spores at various concentrations (0−10 mg/mL) for 24, 48, and 72 h, microscopic examination of L929 cells at 48 h incubation with treated spores at 0, 0.00001, 0.0001, 0.001, 0.01, 0.1, 1.0, and 10 mg/mL, and microscopic examination of L929 cells at 48 h incubation with pure SIOs at various dilution titers: 0, 1:1280, 1:640, 1:320, 1:160, 1:80, 1:40, and 1:20 (PDF)

■ AUTHOR INFORMATION

Corresponding Authors

Duangporn Polpanich − *National Nanotechnology Center (NANOTEC), National Science and Technology Development Agency (NSTDA), Pathum Thani 12120, Thailand;* orcid.org/0000-0002-7539-0467; Email: duangporn@nanotec.or.th

Chariya Kaewsaneha − *School of Integrated Science and Innovation, Sirindhorn International Institute of Technology (SIIT), Thammasat University, Pathum Thani 12121, Thailand;* orcid.org/0000-0003-2758-8388; Email: chariya@siit.tu.ac.th

Authors

Bunthoeurn Khann − *School of Integrated Science and Innovation, Sirindhorn International Institute of Technology (SIIT), Thammasat University, Pathum Thani 12121, Thailand*

Pakorn Opaprakasit − *School of Integrated Science and Innovation, Sirindhorn International Institute of Technology (SIIT), Thammasat University, Pathum Thani 12121, Thailand;* orcid.org/0000-0003-1490-8258

Yodsathorn Wongngam − *National Nanotechnology Center (NANOTEC), National Science and Technology Development Agency (NSTDA), Pathum Thani 12120, Thailand;* orcid.org/0000-0002-6338-3008

Kamonchanok Thananukul − *School of Integrated Science and Innovation, Sirindhorn International Institute of Technology (SIIT), Thammasat University, Pathum Thani 12121, Thailand*

Complete contact information is available at: https://pubs.acs.org/10.1021/acsomega.3c01698

https://doi.org/10.1021/acsomega.3c01698
ACS Omega 2023, 8, 20937−20948

Notes

The authors declare no competing financial interest.

■ ACKNOWLEDGMENTS

This study is supported by Thammasat University Research Fund, contract no. TUFT 87/2564 and the NSRF via the Program Management Unit for Human Resources & Institutional Development, Research and Innovation (grant no B16F640084). The authors thank the Center of Excellence in Materials and Plasma Technology (CoE M@P Tech), Thammasat University. The scholarship support from the TAIST-Tokyo Tech program to B.K. is gratefully acknowledged.

■ REFERENCES

(1) Sargin, I.; Akyuz, L.; Kaya, M.; Tan, G.; Ceter, T.; Yildirim, K.; Ertosun, S.; Aydin, G. H.; Topal, M. Controlled release and antiproliferative effect of imatinib mesylate loaded sporopollenin microcapsules extracted from pollens of Betula pendula. *Int. J. Biol. Macromol.* **2017**, *105*, 749−756.

(2) Potroz, M. G.; Mundargi, R. C.; Gillissen, J. J.; Tan, E.-L.; Meker, S.; Park, J. H.; Jung, H.; Park, S.; Cho, D.; Bang, S.-I.; Cho, N.-J. Plant-based hollow microcapsules for oral delivery applications: Toward optimized loading and controlled release. *Adv. Funct. Mater.* **2017**, *27*, 1700270.

(3) Mundargi, R. C.; Potroz, M. G.; Park, S.; Park, J. H.; Shirahama, H.; Lee, J. H.; Seo, J.; Cho, N.-J. Lycopodium spores: A naturally manufactured, superrobust biomaterial for drug delivery. *Adv. Funct. Mater.* **2016**, *26*, 487−497.

(4) Mundargi, R. C.; Tan, E.-L.; Seo, J.; Cho, N.-J. Encapsulation and controlled release formulations of 5-fluorouracil from natural Lycopodium clavatum spores. *J. Ind. Eng. Chem.* **2016**, *36*, 102−108.

(5) Aguiar, M. C. S.; das Gracas Fernandes da Silva, M. F.; Fernandes, J. B.; Forim, M. R. Evaluation of the microencapsulation of orange essential oil in biopolymers by using a spray-drying process. *Sci. Rep.* **2020**, *10*, 11799.

(6) Gadermaier, G.; Hauser, M.; Ferreira, F. Allergens of weed pollen: an overview on recombinant and natural molecules. *Methods* **2014**, *66*, 55−66.

(7) Diego-Taboada, A.; Beckett, S. T.; Atkin, S. L.; Mackenzie, G. Hollow pollen shells to enhance drug delivery. *Pharmaceutics* **2014**, *6*, 80−96.

(8) Atkin, S. L.; Barrier, S.; Cui, Z.; Fletcher, P. D.; Mackenzie, G.; Panel, V.; Sol, V.; Zhang, X. UV and visible light screening by individual sporopollenin exines derived from Lycopodium clavatum (club moss) and Ambrosia trifida (giant ragweed). *J. Photochem. Photobiol., B* **2011**, *102*, 209−217.

(9) Mundargi, R. C.; Potroz, M. G.; Park, J. H.; Seo, J.; Lee, J. H.; Cho, N.-J. Extraction of sporopollenin exine capsules from sunflower pollen grains. *RSC Adv.* **2016**, *6*, 16533−16539.

(10) Fan, T.; Park, J. H.; Pham, Q. A.; Tan, E. L.; Potroz, M. G.; Mundargi, R. C.; Potroz, M. G.; Jung, H.; Cho, N. J. Extraction of cage-like sporopollenin exine capsules from dandelion pollen grains. *Sci. Rep.* **2018**, *8*, 6565.

(11) Mundargi, R. C.; Potroz, M. G.; Park, J. H.; Seo, J.; Tan, E. L.; Cho, N.-J.; Lee, J. H.; Cho, N. J. Eco-friendly streamlined process for sporopollenin exine capsule extraction. *Sci. Rep.* **2016**, *6*, 19960.

(12) Prabhakar, A. K.; Lai, H. Y.; Potroz, M. G.; Corliss, M. K.; Park, J. H.; Mundargi, R. C.; Cho, D.; Bang, S. I.; Cho, N. J. Chemical processing strategies to obtain sporopollenin exine capsules from multi-compartmental pine pollen. *J. Ind. Eng. Chem.* **2017**, *53*, 375−385.

(13) Uddin, M. J.; Liyanage, S.; Abidi, N.; Gill, H. S. Physical and biochemical characterization of chemically treated pollen shells for potential use in oral delivery of therapeutics. *J. Pharm. Sci.* **2018**, *107*, 3047−3059.

(14) Barrier, S.; Diego-Taboada, A.; Thomasson, M. J.; Madden, L.; Pointon, J. C.; Wadhawan, J. D.; Beckett, S. T.; Atkin, S. L.; Mackenzie, G. Viability of plant spore exine capsules for microencapsulation. *J. Mater. Chem.* **2011**, *21*, 975−981.

(15) Diego-Taboada, A.; Maillet, L.; Banoub, J. H.; Lorch, M.; Rigby, A. S.; Boa, A. N.; Atkin, S. L.; Mackenzie, G. Protein free microcapsules obtained from plant spores as a model for drug delivery: ibuprofen encapsulation, release and taste masking. *J. Mater. Chem. B* **2013**, *1*, 707−713.

(16) Wu, D.; Liang, Y.; Pei, Y.; Li, B.; Liang, H. Plant exine capsules based encapsulation strategy: A high loading and long-term effective delivery system for nobiletin. *Food Res. Int.* **2020**, *127*, 108691.

(17) Taha, N. F.; Dyab, A. K. F.; Emara, L. H.; Meligi, N. M. Microencapsulation of diclofenac sodium into natural Lycopodium clavatum spores: In vitro release and gastro-ulcerogenic evaluations. *J. Drug Deliv. Sci. Technol.* **2022**, *71*, 103278.

(18) Dyab, A. K. F.; Mohamed, M. A.; Meligi, N. M.; Mohamed, S. K. Encapsulation of erythromycin and bacitracin antibiotics into natural sporopollenin microcapsules: antibacterial, cytotoxicity, in vitro and in vivo release studies for enhanced bioavailability. *RSC Adv.* **2018**, *8*, 33432−33444.

(19) Alpizar-Reyes, E.; Concha, J. L.; Martin-Martinez, F. J.; Norambuena-Contreras, J. Biobased spore icrocapsules for asphalt self-healing. *ACS Appl. Mater. Interfaces* **2022**, *14*, 31296−31311.

(20) Fanali, C.; Dugo, L.; Cacciola, F.; Beccaria, M.; Grasso, S.; Dacha, M.; Dugo, P.; Mondello, L. Chemical characterization of sacha inchi (Plukenetia volubilis L.) oil. *J. Agric. Food Chem.* **2011**, *59*, 13043−13049.

(21) Elgegren, M.; Kim, S.; Cordova, D.; Silva, C.; Noro, J.; Cavaco-Paulo, A.; Nakamatsu, J. Ultrasound-assisted encapsulation of Sacha Inchi (Plukenetia volubilis Linneo.) oil in alginate-chitosan nanoparticles. *Polymers* **2019**, *11*, 1245.

(22) Chirinos, R.; Zuloeta, G.; Pedreschi, R.; Mignolet, E.; Larondelle, Y.; Campos, D. Sacha inchi (Plukenetia volubilis): a seed source of polyunsaturated fatty acids, tocopherols, phytosterols, phenolic compounds and antioxidant capacity. *Food Chem.* **2013**, *141*, 1732−1739.

(23) Gonzalez-Aspajo, G.; Belkhelfa, H.; Haddioui-Hbabi, L.; Bourdy, G.; Deharo, E. Sacha inchi oil (Plukenetia volubilis L.), effect on adherence of Staphylococus aureus to human skin explant and keratinocytes in vitro. *J. Ethnopharmacol.* **2015**, *171*, 330−334.

(24) Gonzales, G. F.; Gonzales, C. A randomized, double-blind placebo-controlled study on acceptability, safety and efficacy of oral administration of sacha inchi oil (Plukenetia volubilis L.) in adult human subjects. *Food Chem. Toxicol.* **2014**, *65*, 168−176.

(25) Soimee, W.; Nakyai, W.; Charoensit, P.; Grandmottet, F.; Worasakwutiphong, S.; Phimnuan, P.; Viyoch, J. Evaluation of moisturizing and irritation potential of sacha inchi oil. *J. Cosmet. Dermatol.* **2020**, *19*, 915−924.

(26) Wang, S.; Zhu, F.; Kakuda, Y. Sacha inchi (Plukenetia volubilis L.): Nutritional composition, biological activity, and uses. *Food Chem.* **2018**, *265*, 316−328.

(27) da Silva Soares, B.; Siqueira, R. P.; de Carvalho, M. G.; Vicente, J.; Garcia-Rojas, E. E. Microencapsulation of sacha inchi oil (Plukenetia volubilis L.) using complex coacervation: Formation and structural characterization. *Food Chem.* **2019**, *298*, 125045.

(28) Silva, K. F. C. e.; da Silva Carvalho, A. G.; Rabelo, R. S.; Hubinger, M. D. Sacha inchi oil encapsulation: Emulsion and alginate beads characterization. *Food Bioprod. Process.* **2019**, *116*, 118−129.

(29) Otalora, M. C.; Camelo, R.; Wilches-Torres, A.; Cardenas-Chaparro, A.; Gomez Castano, J. A. Encapsulation effect on the in vitro bioaccessibility of sacha inchi oil (Plukenetia volubilis L.) by soft capsules composed of gelatin and cactus mucilage biopolymers. *Polymers* **2020**, *12*, 1995.

(30) El Ghazzaqui Barbosa, A.; Constantino, A. B. T.; Bastos, L. P. H.; Garcia-Rojas, E. E. Encapsulation of sacha inchi oil in complex coacervates formed by carboxymethylcellulose and lactoferrin for controlled release of β-carotene. *Food Hydrocolloids Health* **2022**, *2*, 100047.

https://doi.org/10.1021/acsomega.3c01698
ACS Omega 2023, 8, 20937−20948

(31) Kaewsaneha, C.; Bitar, A.; Tangboriboonrat, P.; Polpanich, D.; Elaissari, A. Fluorescent-magnetic Janus particles prepared via seed emulsion polymerization. *J. Colloid Interface Sci.* **2014**, *424*, 98−103.
(32) Gonzalez-Cruz, P.; Uddin, M. J.; Atwe, S. U.; Abidi, N.; Gill, H. S. A chemical treatment method for obtaining clean and intact pollen shells of different species. *ACS Biomater. Sci. Eng.* **2018**, *4*, 2319−2329.
(33) Deng, Z.; Pei, Y.; Wang, S.; Zhou, B.; Li, J.; Hou, X.; Li, J.; Li, B.; Liang, H. Carboxymethylpachymaran entrapped plant-based hollow microcapsules for delivery and stabilization of beta-galactosidase. *Food Funct.* **2019**, *10*, 4782−4791.
(34) Bastos, L. P. H.; Dos Santos, C. H. C.; de Carvalho, M. G.; Garcia-Rojas, E. E. Encapsulation of the black pepper (Piper nigrum L.) essential oil by lactoferrin-sodium alginate complex coacervates: Structural characterization and simulated gastrointestinal conditions. *Food Chem.* **2020**, *316*, 126345.
(35) Diego-Taboada, A.; Cousson, P.; Raynaud, E.; Huang, Y.; Lorch, M.; Binks, B. P.; Queneau, Y.; Boa, A. N.; Atkin, S. L.; Beckett, S. T.; Mackenzie, G. Sequestration of edible oil from emulsions using new single and double layered microcapsules from plant spores. *J. Mater. Chem.* **2012**, *22*, 9767.
(36) Ji, Y.; Yang, X.; Ji, Z.; Zhu, L.; Ma, N.; Chen, D.; Jia, X.; Tang, J.; Cao, Y. DFT-calculated IR spectrum amide I, II, and III band contributions of N-methylacetamide fine components. *ACS Omega* **2020**, *5*, 8572−8578.
(37) Uddin, M. J.; Abidi, N.; Warzywoda, J.; Gill, H. S. Investigation of the fate of Proteins and hydrophilicity/hydrophobicity of Lycopodium clavatum spores after organic solvent-base-acid treatment. *ACS Appl. Mater. Interfaces* **2019**, *11*, 20628−20641.
(38) Archibald, S. J.; Atkin, S. L.; Bras, W.; Diego-Taboada, A.; Mackenzie, G.; Mosselmans, J. F. W.; Nikitenko, S.; Quinn, P. D.; Thomas, M. F.; Young, N. A. How does iron interact with sporopollenin exine capsules? An X-ray absorption study including microfocus XANES and XRF imaging. *J. Mater. Chem. B* **2014**, *2*, 945−959.
(39) Vukmirović, S.; Ilić, V.; Tadić, V.; Čapo, I.; Pavlović, N.; Tomas, A.; Paut Kusturica, M.; Tomić, N.; Maksimović, S.; Stilinović, N. Comprehensive analysis of antioxidant and hepatoprotective properties of morus nigra L. *Antioxidants* **2023**, *12*, 382.
(40) Traber, M. G.; Stevens, J. F. Vitamins C and E: beneficial effects from a mechanistic perspective. *Free Radic. Biol. Med.* **2011**, *51*, 1000−1013.
(41) Thomasson, M. J.; Diego-Taboada, A.; Barrier, S.; Martin-Guyout, J.; Amedjou, E.; Atkin, S. L.; Queneau, Y.; Boa, A. N.; Mackenzie, G. Sporopollenin exine capsules (SpECs) derived from Lycopodium clavatum provide practical antioxidant properties by retarding rancidification of an ω-3 oil. *Ind. Crops Prod.* **2020**, *154*, 112714.
(42) Atwe, S. U.; Ma, Y.; Gill, H. S. Pollen grains for oral vaccination. *J. Control. Release* **2014**, *194*, 45−52.
(43) Mitsumoto, K.; Yabusaki, K.; Aoyagi, H. Classification of pollen species using autofluorescence image analysis. *J. Biosci. Bioeng.* **2009**, *107*, 90−94.
(44) Roshchina, V. V. Vital Autofluorescence: Application to the Study of Plant Living Cells. *Int. J. Spectrosc.* **2012**, *2012*, 124672.
(45) Gutierrez, L. F.; Quinones-Segura, Y.; Sanchez-Reinoso, Z.; Diaz, D. L.; Abril, J. I. Physicochemical properties of oils extracted from gamma-irradiated Sacha Inchi (Plukenetia volubilis L.) seeds. *Food Chem.* **2017**, *237*, 581−587.
(46) Thananukul, K.; Kaewsaneha, C.; Sreearunothai, P.; Petchsuk, A.; Buchatip, S.; Supmak, W.; Nim, B.; Okubo, M.; Opaprakasit, P. Biocompatible degradable hollow nanoparticles from curable copolymers of polylactic acid for UV-shielding cosmetics. *ACS Appl. Nano Mater.* **2022**, *5*, 4473−4483.
(47) Kerr, J. B.; Fioletov, V. E. Surface ultraviolet radiation. *Atmos. Ocean.* **2008**, *46*, 159−184.
(48) Esparza, Y.; Ngo, T.-D.; Boluk, Y. Preparation of powdered oil particles by spray drying of cellulose nanocrystals stabilized Pickering hempseed oil emulsions. *Colloids Surf., A* **2020**, *598*, 124823.
(49) Alpizar-Reyes, E.; Varela-Guerrero, V.; Cruz-Olivares, J.; Carrillo-Navas, H.; Alvarez-Ramirez, J.; Perez-Alonso, C. Microencapsulation of sesame seed oil by tamarind seed mucilage. *Int. J. Biol. Macromol.* **2020**, *145*, 207−215.
(50) *Biological Evaluation of Medical Devices-Part 5: Tests for In Vitro Cytotoxicity*, 1999; pp 1−8. ISO 10993.
(51) Bucur, M.; Constantin, C.; Neagu, M.; Zurac, S.; Dinca, O.; Vladan, C.; Cioplea, M.; Popp, C.; Nichita, L.; Ionescu, E. Alveolar blood clots and platelet-rich fibrin induce in vitro fibroblast proliferation and migration. *Exp. Ther. Med.* **2018**, *17*, 982−989.

https://doi.org/10.1021/acsomega.3c01698
ACS Omega 2023, 8, 20937−20948